Multi-GNSS Receiver Antenna Calibration

Johannes KRÖGER, Tobias KERSTEN, Yannick BREVA, and Steffen SCHÖN, Germany

Key words: antenna calibration, phase center corrections, Multi-GNSS, Multi-Frequency

SUMMARY

Global Navigation Satellite Systems (GNSS) are not only widely used for precise positioning, navigation and timing but also for establishing of terrestrial reference frames for geospatial applications, such as land and water management.
The quality of GNSS carrier phase measurements depends on the knowledge about the location of the exact electrical reception point of the GNSS receiver antenna, also known as phase center. Because the location of this receiving point varies with the direction of the incoming satellite signal, phase center corrections (PCC), including a phase center offset (PCO) and phase center variations (PCV), have to be taken into account. These corrections are determined by a calibration of the antennas either in an anechoic chamber using artificially generated signals or in the field by use of a robot and real GNSS signals. The frequency dependent PCC are published in the IGS Antenna Exchange format (ANTEX).

In order to take the benefits from the higher quality of the newer frequencies (like GPS L5) and satellite systems (e.g. Galileo or Beidou) so that multi-GNSS measurements can be processed, PCC have to be provided also for these signals.
In this contribution, the calibration procedure developed at the Institut für Erdmessung (IfE) is presented. The robot model as well as the data acquisition and analysis is shown. Furthermore, the estimation process of the PCC using spherical harmonics is explained in details.
We show, that an absolute GNSS receiver antenna calibration using a robot and real signals can successfully be carried out at the Institut für Erdmessung (IfE). The results underline an overall good repeatability with an RMS for the difference patterns of different calibrations smaller than two millimeters. It is shown that the L5 patterns significantly vary from L2, so that specific calibration values are needed. In addition, the concept of a joint estimation approach of same frequencies (like GPS L1 and Galileo L1) and its difference to the "classical" approach of frequency and system dependent pattern is presented. It can be seen, that differences up to 5.5 mm are present, if the joint estimated PCC are compared to the "classical" EL1X PCC. This underlines the demand of not only frequency but also GNSS specific PCC.

Multi-GNSS Receiver Antenna Calibration

Johannes KRÖGER, Tobias KERSTEN, Yannick BREVA, and Steffen SCHÖN, Germany

1. Introduction

Global Navigation Satellite Systems (GNSS) are not only widely used for precise positioning, navigation and timing (PNT) but also for the realization of geodetic reference frames which are strongly needed for geospatial applications like land and water management (Altamimi, et al., 2016).
Currently, four GNSS in medium earth orbiter constellation (MEO) are available, namely the U.S. Global Positioning System (GPS), the European Galileo, the Russian GLONASS and the Chinese Beidou system. In addition, regional constellations like the Indian Regional Navigation Satellite System (IRNSS) or the Japanese Quasi Zenith Satellite System (QZSS) complete the various systems. As multi-GNSS processing increases the accuracy of the application related solutions or even make only a processing possible (e.g. in dense urban areas), it has become a key factor nowadays.
Consequently, the quality of the GNSS phase measurement depends, among other factors, on the knowledge of the exact electrical receiving point of the GNSS receiver antenna, the so-called carrier phase center.
Because receiving antennas are designed as a compromise of various physical parameters (e.g. gain, multipath reduction, weight and size, etc.), the electrical phase center - the geometric location to which the actual phase measurement refers - varies with the direction of the satellite signal and thus deviates from an ideal omnidirectional radiation pattern (Rao, et al., 2013; Stutzman & Thiele, 2012).

Nowadays, phase center corrections (PCC) are determined either in an anechoic chamber using artificial generated signals (Görres, et al., 2006; Zeimetz & Kuhlmann, 2008; Becker, et al., 2010) or in the field by a precisely calibrated robot (Menge, et al., 1998; Wübbena, et al., 2000; Böder, et al., 2001; Seeber & Böder, 2002). The research presented in this paper is based on the robot approach that is implemented by our group at the Institut für Erdmessung (IfE) as part of our in-house GNSS toolbox to meet the requirements for estimating multi-GNSS PCC for additional satellite systems (Kersten & Schön, 2010; Kersten, 2014). This implemented concept serves as an independent solution strategy other than explained by Wübbena, et al., (2019).

In order to obtain high-precision measurements, PCC are required. A set of PCC is a unique composition of a phase center offset (PCO) projected onto the line-of-sight (LOS) unit vector $\vec{e}$ to satellite k and phase center variations (PCV) that depend on azimuth α and zenith angle z like

$$PCC(\alpha, z) = -PCO \cdot \vec{e}\,(\alpha^k, z^k) + PCV(\alpha^k, z^k) + r. \quad (1)$$

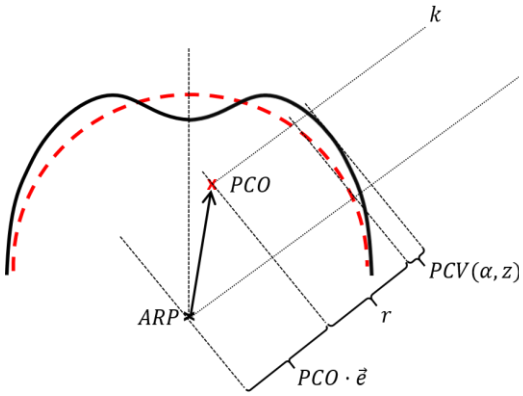

Figure 1: Geometrical interpretation of PCC. The red dashed line shows the theoretical omnidirectional radiation pattern of a GNSS receiver antenna. The black line indicates the real phase front. Differences are defined as PCC.

Since GNSS observations are of relative character, a constant part r is also present (cf. Eq. 1). Due to the constant nature of r, its separation from the receiver clock error is not possible. Thus, a datum is required.

Generally, one restriction could be applied to define PCC in zenith to be equal to 0 (zero zenith condition). Another restriction is setting up a zero mean condition - either over parts or over the whole hemisphere. Figure 1 depicts the geometrical interpretation of the PCC, which corrects the observations for the differences between the ideal and the real phase front.

Currently, one of the most difficult issues in using all GNSS is the lack of a consistent multi-frequency multi-GNSS PCC. For receiving antennas only GPS and GLONASS L1 and L2 frequencies are officially published in the Antenna Exchange (ANTEX) (Rothacher & Schmid, 2010) format by the International GNSS Service (IGS) (Johnston, et al., 2017; IGS, 2019). Here, the majority of calibration values are from method robot. Individual calibration from method chamber are in use for 34 antennas in the European Permanent Network (EPN) (Bruyninx & Legrand, 2017; Bruyninx, et al., 2019). At present, the inconsistent composition of PCC from different calibration methods is still a challenge and should be prevented if possible, as studies on the length and orientation of the different baselines show (Kersten, et al., 2019).

The organisation of the paper is as follows. In Sec. 2 the developed calibration method at IfE is presented. This contains the data acquisition, the data pre-processing and the estimation of the PCC. Section 3 shows calibration results for different geodetic antennas. In Sec. 4 the repeatability of the calibration strategy is analysed and the obtained PCC compared to a set of PCC from the latest IGS Repro3 ANTEX version. Section 5 presents the idea of a joint estimation approach for similar frequencies of different GNSS. We present first results and the differences to the standard estimation approach. Section 6 closes the paper with the conclusion.

2. Calibration method

In order to estimate PCC, robot with 5 degrees of freedom is used to rote and tilt the antenna under test (AUT) precisely within $\Delta t \approx 1\ s$ around a fixed point in space. The re-positioning accuracy obtained from different orientation of the robot unit is about 0.25 mm (Kersten, 2014). At a distance of approximately 8 m, a reference station is located equipped with a

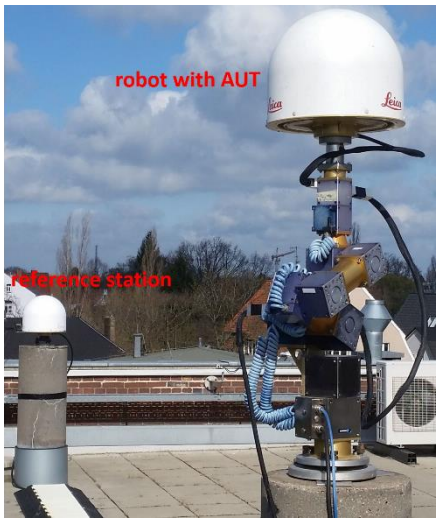

Figure 2: Calibration set-up at IfE. In the foreground the robot with the AUT can be seen. At a distance of approximately 8 m the reference station is located.

geodetic choke ring antenna (LEIAR25.R3). Identical receivers are in use at both stations connected to a common external frequency standard (Standard Rubidium FS725) with a stability of $< 2 \cdot 10^{-11}$ (Kersten, 2014). Hence, the individual receiver clock drift is identical at both receivers and cancels out if generating receiver-to-receiver single differences (SD). Figure 2 shows the calibration set-up on our GNSS rooftop at IfE.
The robot tilts and rotates the AUT with defined sequences whereas the sequence depends on the actual GPS satellite constellation. The investigated concept is a post processing approach. Here, logging movements of the robot w.r.t. corresponding timestamps as well as the GNSS raw data during the calibration defines the fundamental basis of our approach. Usually, a standard calibration takes about 4 hours.
In order to prepare the recorded raw data for the PCC estimation, a data pre-processing is required after the calibration. The actual position of the AUT using a robot model with its defined arm lengths and the remaining robot module offsets are calculated. The robot model was determined with a laser scanner (Kersten, 2014). Subsequently, the data is transformed into the antenna frame. SD are computed in order to cancel out most of the GNSS error budget on this short baseline including signal propagation errors due to ionospheric or tropospheric effects, orbital errors and common parts of the receiver clock error. Generating time-differenced SD (dSD) removes the ambiguity term as well as the impact of the PCC of the reference antenna. Moreover, the short time intervals between subsequent epochs strongly reduce multipath effects as the relative geometry between the satellite and the station does not change significantly in this minimal timespan. Finally, the phase-wind up (PWU) effect (Wu, et al., 1993) is computed for the AUT so that subsequently the corrected dSD only contain the PCC of the AUT and noise ϵ

$$dSD^k = PCC^k_{AUT}(t_{i+1}) - PCC^k_{AUT}(t_i) + \epsilon(t_i, t_{i+1}). \quad (2)$$

The PCC are parameterized by spherical harmonics (SH) up to degree m = 8 and order n = 8

$$PCC(\alpha^k, z^k) = \sum_{m=1}^{m_{max}} \sum_{n=0}^{m} \widetilde{P_{mn}}(cos\, z^k) \cdot (a_{mn} cos(n\, \alpha^k) + b_{mn} sin(n\, \alpha^k)) \quad (3)$$

with $\tilde{P}$ denoting the fully normalized Legendre function, z^k and α^k being the zenith and azimuth angle in the antenna frame to satellite k, and $a_{mn}$and b_{mn} the unknown parameters.

The unknowns are solved for in a least-squares adjustment

$$\hat{x} = (A^T P A)^{-1} \cdot A^T P\, l. \quad (4)$$

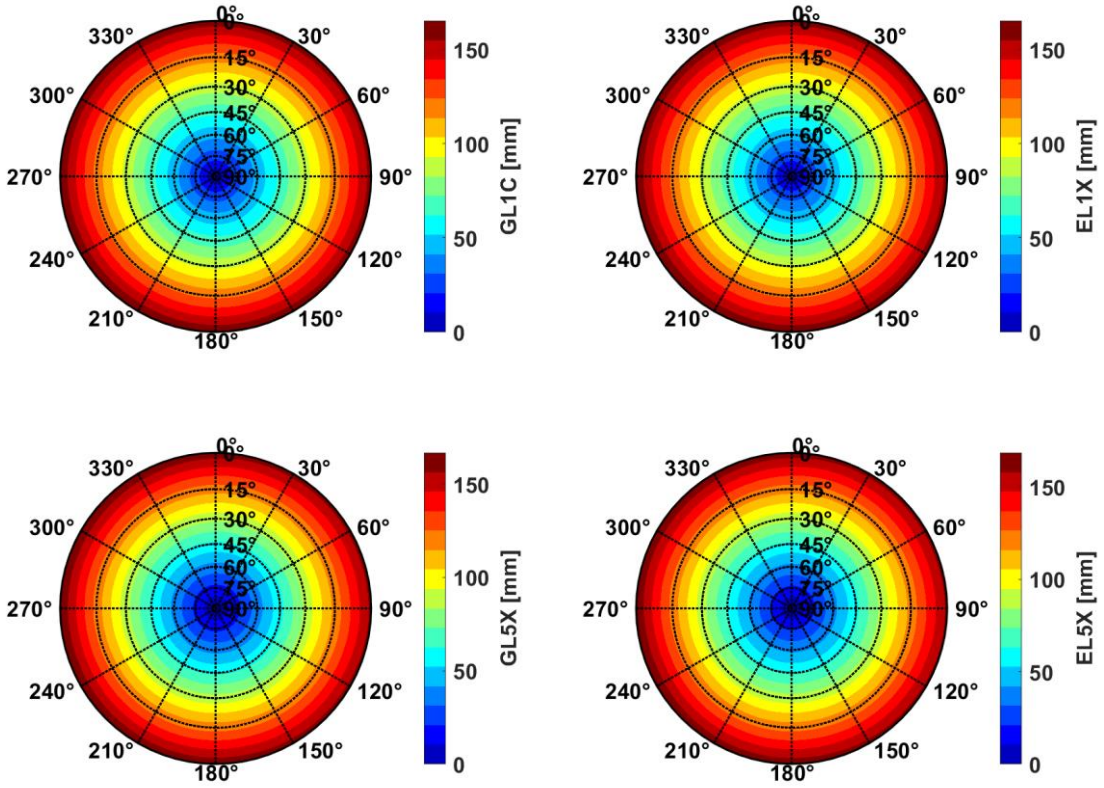

Figure 3: PCC for LEIAR25.R3 LEIT for GL1C, EL1X, GL5X and EL5X.

Here, **A** denotes the design matrix and **P** the weighting matrix and l is the observation vector that contains the observables (dSD) for the estimation step. The design matrix **A** is set up epochwise for each satellite so that the normal equation matrix **N** reads

$$N_k = A_k^T P_k A_k \tag{5}$$

that results in a summation over all satellites.
The condition of the system of equation system is poor as only observations on the antenna hemisphere are available. Consequently, coefficients $a_{mn}$and $b_{mn}$with an odd index sum, such as a_{21}, b_{21} or a_{30}, are restricted to zero since they express the antisymmetric behaviour between the upper and lower half of the sphere.
Next, a synthesis using the estimated unknowns with Eq. 3 results in the grid values to fill the entries of the ANTEX format.

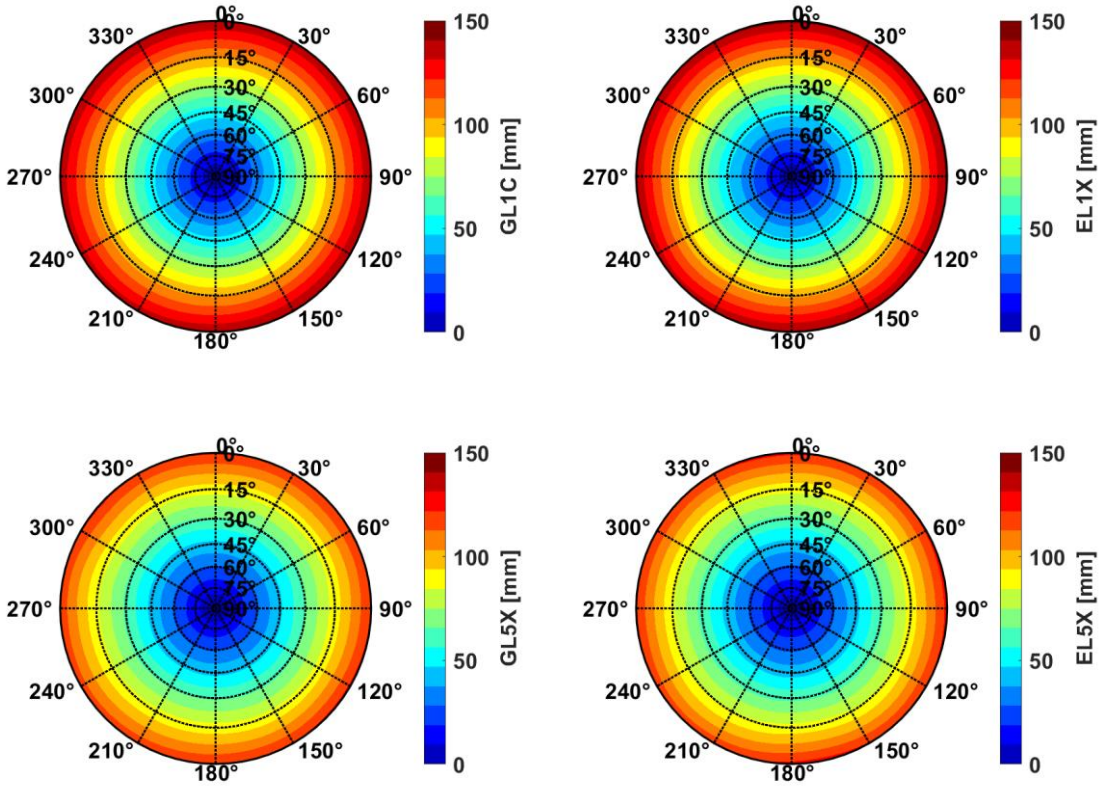

Figure 4: PCC for LEIAR20 LEIM for GL1C, EL1X, GL5X and EL5X.

3. Estimated PCC

During February and August 2019 several calibrations of different antennas and antenna types have been carried out. Figure 3 shows the estimated PCC (including PCO and PCV) of LEIAR25.R3 LEIT antenna for GPS and Galileo frequencies L1 and L5.
The PCC of this geodetic antenna, which is often used for reference stations or high precision applications, are in a range of up to 15 cm and show elevation dependent and only marginally azimuth dependent variations.
Figure 4 depicts the PCC of the antenna LEIAR20 LEIM. The PCC show a very similar behaviour compared to the PCC of LEIAR25.R3. The magnitude of the PCC are slightly smaller.

4. Repeatability and Comparison

In order to analyse the repeatability of estimated PCC, several calibrations have been carried out in August 2019. When different sets of PCC (ΔPCC) for the same antenna or antenna type are compared, it is mandatory to take differences in PCO and different datum definitions correctly into account (Schön und Kersten 2013). As the datum definition is generally not reported, datum independent measures should be used to compare ΔPCC. Subsequently,

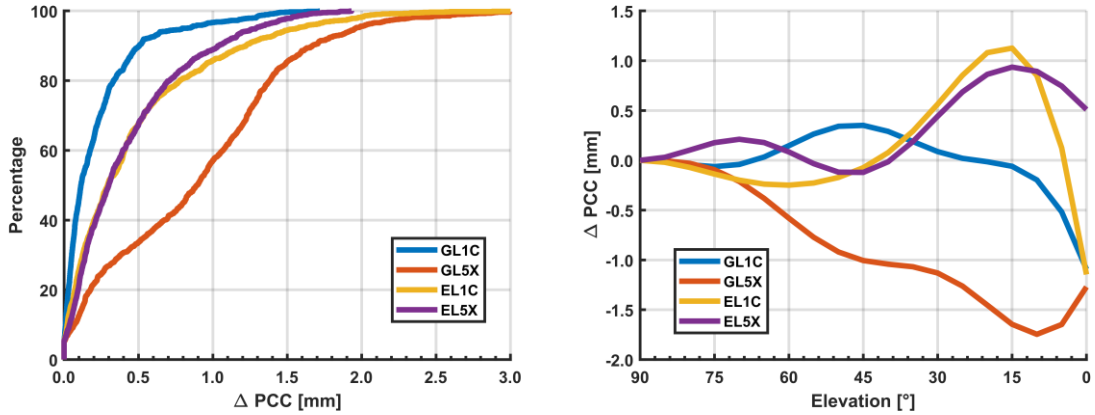

Figure 5: ΔPCC by different calibrations of the same antenna (LEIAR25.R3 LEIT)

(Schön und Kersten 2014) especially propose the spread $\left((PCC_{1_{max}} - PCC_{1_{min}}) - (PCC_{2_{max}} - PCC_{1_{min}})\right)$ to compare ΔPCC.

Figure 5 (left side) shows the absolute cumulative histogram of the ΔPCC for LEIAR25.R3 LEIT between to individual calibrations carried out on DOY239. For both calibrations the same receivers and receiver settings have been used. Since the exact sequence of the robot movements are optimized for the actual GPS constellation and the calibrations were performed approximately with a time difference of 4 hours, the robot poses are not exactly the same.
It can be seen, that the highest difference occur on the GPS L5 signal (GL5X), where 95 % of the differences are below 2 mm. The reason for these higher differences are the less number of satellites transmitting this rather new frequency (only 12 instead of 31 for GPS L1 (Montenbruck, Steigenberger und Prange, et al. 2017). For the other investigated frequencies, 95 % of the ΔPCC are below 1.6 mm and 0.9 mm.
Figure 5 (right side) shows the elevation dependent ΔPCC of the same antenna for two different calibrations. Again, the highest differences are present for GL5X as they are up to 1.7 mm. Due to the zero zenith constraint, the highest frequency specific differences occur in low elevations. Furthermore, a quite similar behaviour of the differences can be observed for EL1C and EL5X. Table 1 gives some numeric values for the ΔPCC. Again, it underlines that the largest differences are present for GL5X since the RMS is higher than 1 mm and the spread almost 2 mm (cf. Fig. 5).

Table 1: Spread and RMS of ΔPCC for LEIAR25.R3 LEIT between two calibrations on DOY239.

	GL1C	**GL5X**	**EL1C**	**EL5X**
Spread of ΔPCC [mm]	0.88	1.86	0.11	1.28
RMS of ΔPCC[mm]	0.35	1.08	0.69	0.58

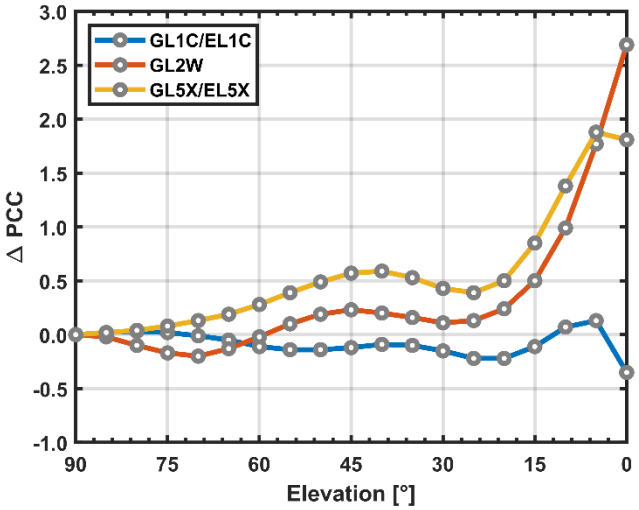

Figure 6: Comparison of individual PCC w.r.t. type mean from LEIAR20 LEIM antenna as part of IGSR3_2077.atx.

Further comparisons of our results are carried out using the current available multi GNSS PCC from the method robot for the recent IGS reprocessing campaign IGS-Repro3 (IGS, 2019). The official name is IGSR3_2077.atx. Here, we analyse the deviations between GPS and Galileo signals and frequencies. Figure 6 presents the corresponding elevation dependent ΔPCC for the antenna LEIAR20 LEIM. The comparison of our individual calibration at IfE w.r.t. the type mean entry of the IGSR3 file shows very good agreement with pure elevation dependent variations of less than 1 mm for the elevations below15° for the cases of GL2W and GL5X/EL5X respectively. An optimal solution is obtained for GL1C as deviations are below 0.5 mm for all elevations. The causes for higher magnitudes for GL2W and GL5X/EL5X below 15° elevation requires further investigation.

5. Joint Estimation approach

Currently, discussions are ongoing if only frequency dependent PCC instead of frequency and system specific PCC should be provided. This would mean, that e.g. for GL1C and EL1C only one set of PCC would be published. A first analysis have been carried out to investigate this question.

Figure 7 presents the ΔPCC between similar frequencies of GPS and Galileo of antenna LEIAR25.R3 (cf. Figure 3). Differences up to 2.3 mm at low elevations are present, whereas the datum independent spread is 1 mm. For L5 the maximum difference is higher with 3.2 mm and the spread is 3.6 mm. Moreover, a difference in the PCO up component with 2.9 mm can be seen. This leads to the conclusion that not only frequency-specific but also system dependent PCC might be provided.

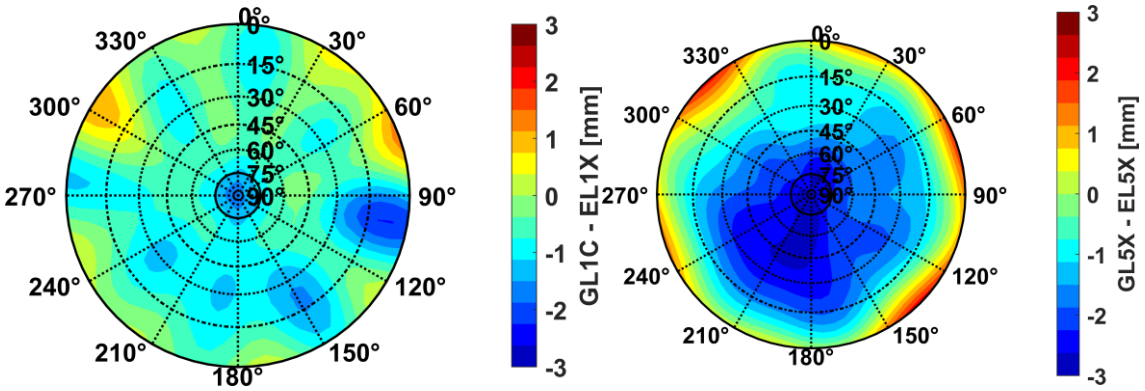

Figure 7: ΔPCC for LEIAR25.R3 LEIT between similar frequencies of different GNSS.

Figure 8 shows the result between the frequencies GL5X and GL2W. Since both frequencies transmit on a similar but not same frequency (L5: 1176.45 MHz, L2: 1227.6 MHz) the question if common PCC for these similar frequencies are adequate should be discussed. It is obvious that differences up to 5.7 mm are present at low elevations. Moreover, a ΔPCO_{UP} of almost 4 mm can be seen. Therefore, it is not adequate to use PCC of L2 for L5 for high precision applications but this was an easy to implement workaround.

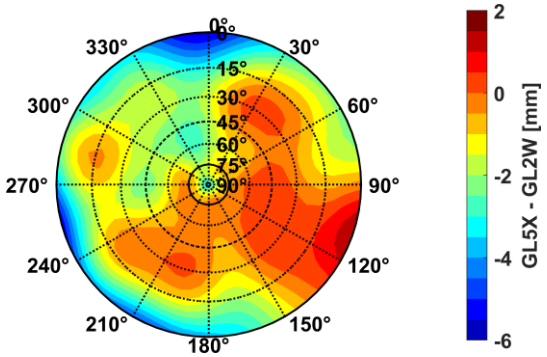

Figure 8: ΔPCC for LEIAR25.R3 LEIT between GL5X and GL2W.

The differences are present, as the PCC have been estimated separately for each GNSS. In a first experimental approach, the PCC for GL1C and EL1C have been estimated together. To this end, the Galileo observations have been added on the level of the normal equation system to the GPS observations.
Figure 9 presents the result of the joint estimation approach for antenna LEIAR25.R3 LEIT for L1, whereas the differences to the standard estimation approach for GL1C and EL1C, respectively, are shown. Note, that for a better visualization different axes limits have been chosen. It can be seen, that the ΔPCC between GL1C and L1 (estimated from GL1C and EL1C) are quite small, i.e. the biggest difference is 0.48 mm (cf. Table 2). The ΔPCC for EL1C-L1 are higher than for Δ(GL1C-L1) and are in a range up to 5.5 mm. Since less observations are present during a standard calibration for Galileo E1 (approx. 26000) compared to GPS L1 (approx. 29000), the smaller

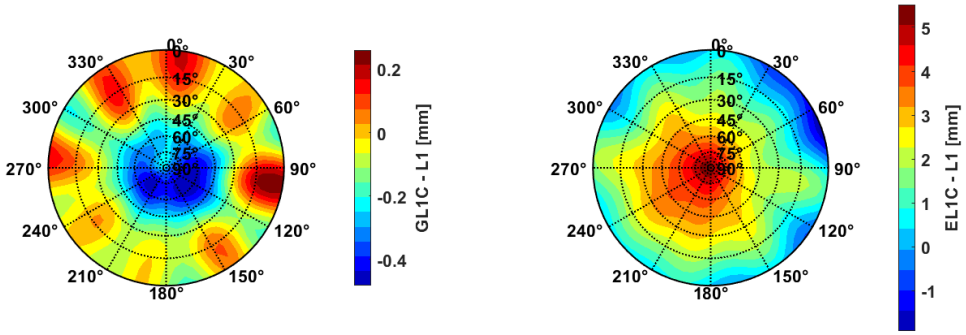

Figure 9: ΔPCC between joint estimated PCC (L1 out of GL1C and EL1C observations) and frequency and system dependent PCC (GL1C and EL1X, respectively).

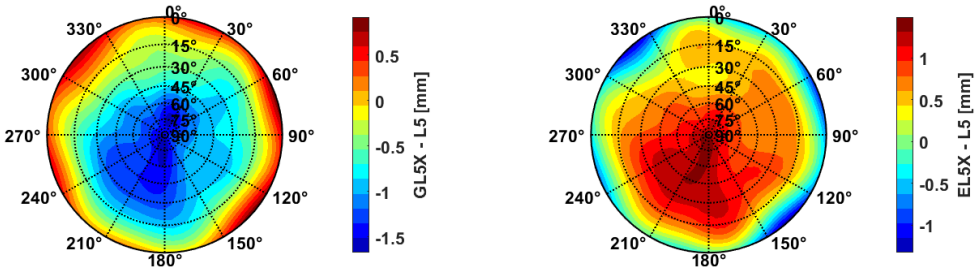

Figure 10: ΔPCC between joint estimated PCC (L5 out of GL5X and EL5X observations) and frequency and system dependent PCC (GL5X and EL5X, respectively).

difference to GL1C could be explained. However, for L5 this is vice versa since more than three times as many observations are present for EL5X (approx. 25800) compared to GL5X (approx.7500). Therefore, the differences are smaller for Δ(EL5X-L5) than for Δ(GL5X-L5), whereas the differences differ not that much (cf. Fig. 10). This issue needs further investigation, e.g. with a validation of the resulting PCC on observation and position domain.

Table 2 gives some numerical values which are related to Fig. 9 and Fig. 10. Again, it can be clearly seen that the differences for Δ(GL1C-L1) are the smallest while for Δ(EL1X-L1) the differences are the highest. However, the maximal ΔPCC is for all cases except GL1C larger than 1 mm which underlines the demand of not only frequency but also GNSS specific PCC.

Table 2: Statistical measures for the joint PCC estimation of similar frequencies but different GNSS.

	Spread [mm]	**RMS [mm]**	**Δmax [mm]**
Δ (GL1C – L1)	0.33	0.26	0.48
Δ (EL1X – L1)	4.91	3.71	5.52
Δ (GL5X – L5)	2.04	1.15	1.67
Δ (EL5X – L5)	1.56	1.02	1.49

6. Conclusion

This contribution presented the developed method at IfE for absolute receiver antenna calibration in the field using a robot. It have been shown that the calibrations show an overall good repeatability with a RMS for the difference PCC smaller than 1.1 mm for all frequencies except GL5X. Additionally, a PCC comparison to the recent ANTEX file have been carried out. The PCC estimated at IfE show a good agreement with the published typemean PCC of this ANTEX version. Here, differences smaller than 1 mm for GL1C/EL1C for all elevation angles and smaller than 1 mm for GL2W and EL5X/EL5X up to an elevation angle of 15° are present.

Furthermore, an analyse have shown that not only frequency but system specific PCC should be provided as the differences of these patterns are in a range up to 5.5 mm for E1 Galileo and 5.7 mm between the similar frequencies L2 and L5.

First results of a joint estimation approach, where PCC with observations from both GPS and Galileo signals is estimated, show maximal differences up to 5.5 mm while the differences between GL1C and L1 are very small.

REFERENCES

Altamimi, Zumeir, Paul Rebischung, Laurent Métivier, and Xavier Collilieux. „ITRF2014: A new release of the International Terrestrial Reference Frame modelling nonlinear station motions.“ *J. Geophys. Res.* (JGR Solid Earth) 121, Nr. 8 (2016).

Becker, Matthias, Phillip Zeimetz, and Erik Schönemann. „Anechoic Chamber calibrations of phase center variations for new and existing GNSS signals and potential impacts in IGS processing.“ *IGS Workshop 2010 and Vertical Rates Symposium, June 28 - July 2, Newcastle upon Tyne, United Kingdom of Great Britain.* 2010.

Böder, Volker, Falko Menge, Günter Seeber, Gerhard Wübbena, and Martin Schmitz. „How to Deal With Station Dependent Errors, New Developments of the Absolute Field Calibration of PCV and Phase-Multipath With a Precise Robot.“ In *Proceedings of the 14th International Technical Meeting of the Satellite Division of The Institute of Navigation (ION GPS 2001), September 11 - 14, Salt Lake City, UT, USA*, 2166-2176. Institute of Navigation (ION), 2001.

Bruyninx, C., and J. Legrand. „Receiver Antenna Calibrations Available from the EPN CB.“ *EUREF AC Workshop, October 25th-26th, Brussels, Belgium.* 2017.

Bruyninx, Carine, Juliette Legrand, András Fabian, and Eric Pottiaux. „GNSS metadata and data validation in the EUREF Permanent Network.“ *GPS Solutions* (Springer Science and Business Media LLC) 23 (8 2019).

Görres, Barbara, James Campbell, Matthias Becker, and M. Siems. „Absolute calibration of GPS antennas: Laboratory results and comparison with field and robot techniques.“ *GPS Solut* 10 (2006): 136-145.

IGS. *Conventions and modelling for repo3.* 10 2019. http://acc.igs.org/repro3/repro3.html.

Johnston, Gary, Anna Riddell, and Grant Hausler. „The International GNSS Service.“ In *Springer Handbook of Global Navigation Satellite Systems*, 967-982. Springer International Publishing, 2017.

Kersten, Tobias. „Bestimmung von Codephasen-Variationen bei GNSS-Empfangsantennen und deren Einfluss auf die Positionierung, Navigation und Zeitübertragung.“ Ph.D.

dissertation, Deutsche Geodätische Kommission (DGK) bei der Bayerischen Akademie der Wissenschaften (BADW), No. 740, 2014.

Kersten, Tobias, Johannes Kröger, Yannick Breva, and Steffen Schön. "Deficiencies of Phase Centre Models: Assessing the impact on geodetic parameters." *Geophysical Research Abstracts 21*. Munich: European Geosciences Union, 2019.

Menge, Falko, Günter Seeber, Christian Völksen, Gerhard Wübbena, and Martin Schmitz. „Results of the absolute field calibration of GPS antenna PCV.“ In *Proceedings of the 11th International Technical Meeting of the Satellite Division of The Institute of Navigation (ION GPS 1998), September 15 - 18, Nashville, TN, USA*, 31-38. Institute of Navigation (ION), 1998.

Montenbruck, Oliver, et al. „IGS-MGEX: Preparing the Ground for Multi-Constellation GNSS Science.“ *4th International Colloquium on Scientific and Fundamental Aspects of the Galileo System, Dezember 4-6, Prague, Czech Republic.* 2013. 8.

Montenbruck, Oliver, et al. „The Multi-GNSS Experiment (MGEX) of the International GNSS Service (IGS) – Achievements, prospects and challenges.“ *Advances in Space Research* (Elsevier BV) 59 (4 2017): 1671-1697.

Rao, B. Rama, Waldemar Kunysz, Ronald L. Fante, and Keith McDonals. *GPS/GNSS Antennas.* Artech House Publishers, Norwood, USA, 2013.

Rothacher, Markus, and Ralf Schmid. „ANTEX: The Antenna Exchange Format, Version 1.4.“ *ftp://igscb.jpl.nasa.gov/igscb/station/general/antex14.txt*, 2010.

Schön, Steffen, and Tobias Kersten. „Comparing antenna phase center corrections: challlenges, concepts and perspectives.“ *IGS Analysis Workshop, June 23.-27., Pasadena, California, USA.* 2014.

—. „On adequate Comparison of Antenna Phase Center Variations.“ *American Geophysical Union, Annual Fall Meeting 2013, December 09.-13., San Francisco, CA, USA.* 2013.

Seeber, Günter, and Volker Böder. „Entwicklung und Erprobung eines Verfahrens zur hochpräzisen Kalibrierung von GPS Antennenaufstellungen - Schlussbericht zum BMBF/DLR Vorhaben 50NA9809/8.“ *Institut für Erdmessung*, 2002.

Stutzman, W. L., and G. A. Thiele. *Antenna Theory and Design.* 3. John Wiley Sons, 2012.

Wübbena, Gerhard, Martin Schmitz, und André Warneke. „Geo++ Absolute Multi Frequency GNSS Antenna Calibration.“ *EUREF Analysis Center (AC) Workshop, October 16-17, Warsaw, Poland.* 2019.

Wübbena, Gerhard, Matrin Schmitz, Falko Menge, Volker Böder, and Günter Seeber. „Automated Absolute Field Calibration of GPS Antennas in Real-Time.“ In *Proceedings of the 13th International Technical Meeting of the Satellite Division of The Institute of Navigation (ION GPS 2000), September 19 - 22., Salt Lake City, UT, USA*, 2512-2522. Institute of Navigation (ION), 2000.

Zeimetz, Phillip, and Heiner Kuhlmann. „On the Accuracy of Absolute GNSS Antenna Calibration and the Conception of a New Anechoic Chamber.“ *Proceedings of the FIG Working Week 2008 - Integrating Generations, June 14-19, Stockholm, Sweden.* 2008. 16.

CONTACTS

Johannes Kröger
Institut für Erdmessung (IfE)
Schneiderberg 50
30167 Hannover
GERMANY
Tel. +49511 762 17693
kroeger@ife.uni-hannover-de
www.ife.uni-hannover.de